PREDICTION FOR THE HE I λ10830Å ABSORPTION WING IN THE COMING EVENT OF ETA CARINAE

Amit Kashi[1] and Noam Soker[1]

ABSTRACT

We propose an explanation to the puzzling appearance of a wide blue absorption wing in the He I λ10830Å P Cygni profile of the massive binary star η Car several months before periastron passage. Our basic assumption is that the colliding winds region is responsible for the blue wing absorption. By fitting observations, we find that the maximum outflow velocity of this absorbing material is ~ 2300 km s^{-1}. We also assume that the secondary star is toward the observer at periastron passage. With a toy-model we achieve two significant results. (1) We show that the semimajor axis orientation we use can account for the appearance and evolution of the wide blue wing under our basic assumption. (2) We predict that the Doppler shift (the edge of the absorption profile) will reach a maximum $0-3$ weeks before periastron passage, and not necessarily exactly at periastron passage or after periastron passage.

Subject headings: (stars:) binaries: general−stars: mass loss−stars: winds, outflows−stars: individual (η Car)

1. INTRODUCTION

There is no boring feature when it comes to the massive binary system η Car. Its $P = 5.54$ yr ($P = 2022.7 \pm 1.3$ d; Damineli et al. 2008a) periodicity has been observed in the radio (Duncan & White 2003), IR (Whitelock et al. 2004), visible (e.g., van Genderen et al. 2006), X-ray (Corcoran 2005), and in many emission and absorption lines (e.g., Damineli et al. 2008a,b). Every orbital cycle the system experiences a spectroscopic event, defined by the fading, or even disappearance, of high-ionization emission lines (e.g., Damineli 1996; Damineli et al. 1998, 2000, 2008a,b; Zanella et al. 1984). The rapid changes in the continuum, lines, and in the X-ray properties (e.g., Martin et al. 2006,a,b; Davidson et al. 2005;

[1]Department of Physics, Technion−Israel Institute of Technology, Haifa 32000 Israel; kashia@physics.technion.ac.il; soker@physics.technion.ac.il.

Nielsen et al. 2007; van Genderen et al. 2006; Damineli et al. 2008b; Corcoran 2005) are assumed to occur near the periastron passages of the highly eccentric, $e \simeq 0.9$, binary orbit (e.g., Hillier et al. 2006).

The He I λ10830Å high excitation line has a complex P Cygni profile, composed of three blue-shifted peaks with significant variations over the cycle (Damineli et al. 1998; 2008b). The emission profile has significant variations over the cycle. The Doppler shifts of the peaks are of relatively low velocities, $|v_{\rm peaks}| < 300$ km s^{-1} (Damineli et al. 2008b). The location of the minimum of the profile (the deepest point in absorption) does not change with orbital phase, and stays at $v_{obs-m} = -570$ km s^{-1}. However, the absorption profile does change. In particular, just before periastron a wide blue wing appear in absorption, reaching ~ -1000 km s^{-1} a month before periastron, and ~ -1800 km s^{-1} at periastron, and the maximum equivalent width of absorption occurs 10 day after periastron passage (Damineli et al. 2008b). Damineli et al. (2008b) approximated the average radial velocity of the absorption profile at half intensity, and found it to change from -640 km s^{-1} before phase zero to -450 km s^{-1} shortly after phase zero.

An additional He I λ10830Å blue absorption feature of up to -1000 km s^{-1}, is observed at several arcseconds from the center in the lobes (Smith 2002). In this paper we refer only to the He I λ10830Å ground measurements of Damineli et al. (2008b). We note that other absorption and emission lines of He I can be formed in different regions in the binary system (see also Kashi & Soker 2007b). In particular, some visible He I lines can be formed in the hot winds of the two stars close to their origin, as compared with the He I λ10830Å that is formed in cooler regions. We show that this cooler region can be the post-shock primary wind. Therefore, different He I lines need not have the same behavior along the orbit.

Because of the winds' very complicated flow structure, when starting this project we limited ourself to build a toy-model in order to achieve two goals: (1) To show that the orientation where the secondary is toward us at periastron ($\omega = 90^\circ$), can be accounted for the development of a wide blue absorption wing starting several weeks before periastron passage. (2) To encourage a nightly observation of the He I λ10830Å close to periastron passage.

2. THE STARS AND THEIR WINDS

The η Car binary parameters used by us are compiled by using results from several different papers (e.g., Ishibashi et al. 1999; Damineli et al. 2000; Corcoran et al. 2001, 2004; Hillier et al. 2001; Pittard & Corcoran 2002; Smith et al. 2004; Verner et al. 2005).

The assumed stellar masses are $M_1 = 120 M_\odot$, $M_2 = 30 M_\odot$, the eccentricity is $e = 0.9$, and the orbital period is $P = 2024$ day. The mass loss rates and terminal speeds are $\dot{M}_1 = 3 \times 10^{-4} M_\odot$ yr^{-1}, $\dot{M}_2 = 10^{-5} M_\odot$ yr^{-1}, $v_{1,\infty} = 500$ km s^{-1} and $v_{2,\infty} = 3000$ km s^{-1}. For these parameters, the half opening angle of the wind-collision cone is $\phi_a \simeq 60^\circ$ (Akashi et al. 2006); because of the orbital motion this angle is not constant, and we calculate it along the orbit in the present paper. For the inclination angle we take $i = 41^\circ$ (Davidson et al. 2001; Smith 2002, 2006).

The primary's wind speed depends on latitude (Smith et al. 2003). The minimum in the He I λ10830Å line profile suggests that the primary's wind speed toward us is $v_{obs-m} = -570$ km s^{-1}. The two winds collide, and form a flow structure, schematically drawn in Figure 1. The two winds go through two respective shock waves, and form a contact discontinuity between them. The contact discontinuity asymptotically forms a conical shell surface. The radiative cooling time of the post-shocked primary's wind is short. The post-shocked primary's wind forms a dense flow along the contact discontinuity, which we refer to as the *conical shell.* Absorption is expected to take place mainly outside the stagnation-point region, and so we approximate the conical shell as an ideal cone.

The He I λ10830Å absorption profile results from He I atoms which absorb from the He I λ10830Å emission line and from the continuum emitted by dust. As we are more interested in the wide wing, the continuum is more relevant to our study. As the system approaches periastron, dust is formed closer and closer to the binary system (Kashi & Soker 2008a). This makes things very complicated, as the conical shell, where the absorbing gas reside according to our model, also changes its size. Some of the dust is formed in the conical shell itself.

Other lines, e.g. $H\alpha$ (Smith et al. 2003), also show some fast blueshifted absorption wings. Some of these wings disappear when the system approaches periastron. This is not a problem for our model, since those lines originate in different regions than where the He I λ10830Å line does (e.g. the $H\alpha$ comes from the primary's wind; Smith et al. 2003). We emphasize again that some He I lines (in particular in the visible band) are formed in different regions than the He I λ10830Å line, and their behavior is different as well.

The binary parameter that is most controversial is the orientation of the semimajor axis−the periastron longitude. Some researchers argue that the secondary (less massive) star is away from us during periastron passages, i.e. an orbital longitude of $\omega = 270^\circ$ (e.g., Nielsen et al. 2007; Damineli et al. 2008b), others argue that the secondary is toward us during periastron passages, $\omega = 90^\circ$ (Falceta-Gonçalves et al. 2005; Abraham et al. 2005; Kashi & Soker 2007b, 2008b), and still different values exist in the literature (Davidson 1997; Smith et al. 2004; Dorland 2007; Henley et al. 2008; Okazaki et al. 2008a). Following

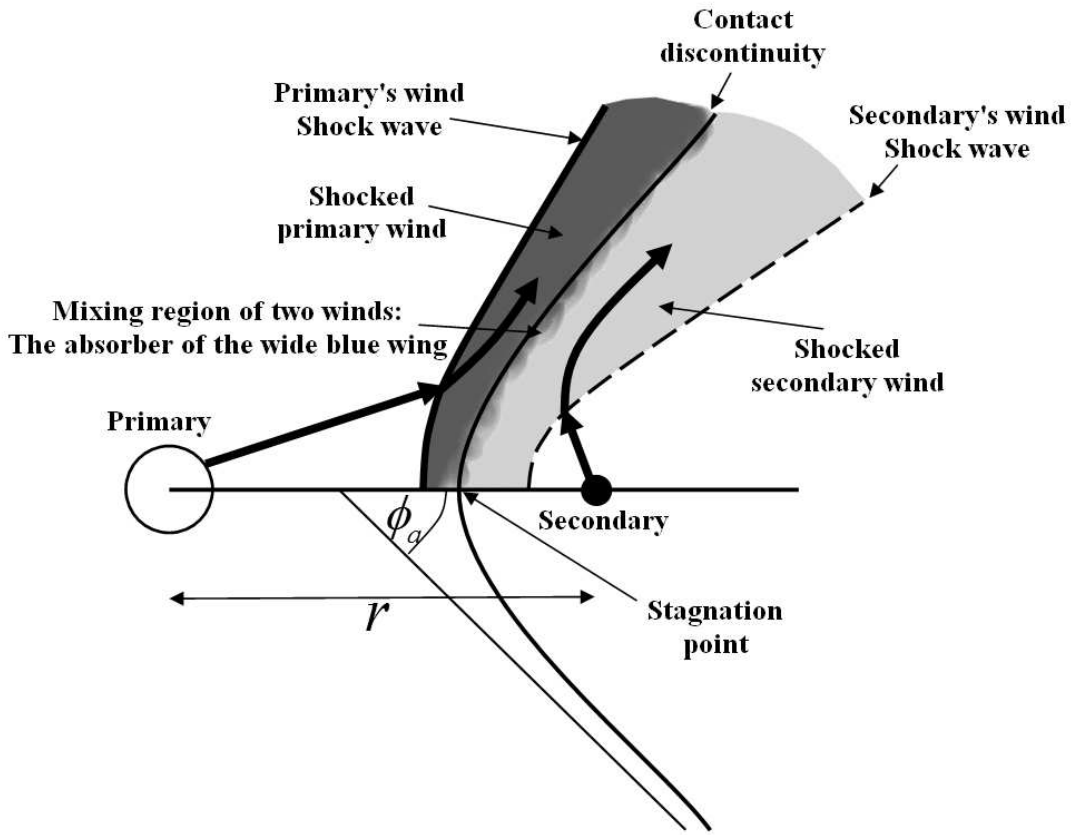

Fig. 1.— The colliding winds structure. The primary's and secondary's winds mix close to the contact discontinuity. According to our models this region is the absorber of the wide He I λ10830Å blue wing. The half opening angle of the wind-collision cone is $\phi_a \simeq 60^\circ$. The thick arrows indicate the flow lines.

our recent paper (Kashi & Soker 2008b) we will take the orientation to be such that the secondary is toward us at periastron ($\omega = 90^\circ$).

3. THE TOY-MODEL

We suggest that the conical shell is responsible for the absorption of the He I λ10830Å high excitation line. When the two winds meet at the contact discontinuity, part of the shocked fast secondary's wind is mixed with part of the shocked slow wind (Pittard 2007), and accelerates part of it to higher velocities. The conical shell has an asymptotic angle of $\phi_a \simeq 60^\circ$, which we take to be the flow direction of the absorbing gas.

In order to make the model more accurate we will take into account the time dependance

of some parameters. The primary's wind velocity profile can be described using the β-profile:

$$v_1(r) = v_s + (v_{1,\infty} - v_s)\left(1 - \frac{R_1}{r}\right)^{\beta}, \tag{1}$$

where $v_s = 20$ km s^{-1} is the sound velocity on the primary's surface, $v_{1,\infty} = 500$ km s^{-1} is the primary's wind terminal velocity, and $\beta = 1$ is a parameter of the wind model.

The radial (along the line joining the two stars) component of the relative velocity between the secondary star and the primary's wind is $v_1 - v_r$, where v_r the radial component of the orbital velocity; v_r is negative when the two stars approach each other. The total relative speed between the secondary and the primary's wind is

$$v_{\rm wind1} = \left[v_\theta^2 + (v_1 - v_r)^2\right]^{1/2}, \tag{2}$$

where v_θ is the tangential component of the orbital velocity. The orbital motion and the variation of the primary wind speed with distance from the primary have a small influence on the conical shell asymptotic angle ϕ_a. We will use the expression given by Eichler & Usov (1993)

$$\phi_a \sim 2.1\left(1 - \frac{\eta^{\frac{4}{5}}}{4}\right)\eta^{\frac{2}{3}}, \tag{3}$$

where

$$\eta \equiv \sqrt{\frac{\dot{M}_2 v_{2,\infty}}{\dot{M}_1 v_{\rm wind1}}}. \tag{4}$$

We will take into consideration the rotation of the cone relatively to the line connecting the two stars. This rotation occurs due to the orbital velocity of the conical shell, and has a considerable influence close to periastron. We define $\delta\phi$ to be the angle measured from the secondary between the direction to the primary and that to the stagnation point (see Soker 2005 for further details)

$$\cos(\delta\phi) = \frac{v_1 - v_r}{v_{\rm wind1}} \tag{5}$$

We find that close to periastron $\delta\phi \simeq 56^\circ$. The geometry and different parameters are shown in Figures 1, 2 and 3.

A closely-related geometry was used by Hill et al. (2000) to fit the excess emission observed in the C III λ5696Å line in the spectra of WR 42 and WR 79. Luehrs (1997) also used a somewhat different geometry to fit the excess emission observed in the C III λ5696Å line in the spectra of WR 79. These two models were purely geometric. In the model we suggest for the absorption, some more considerations have to be taken in to account.

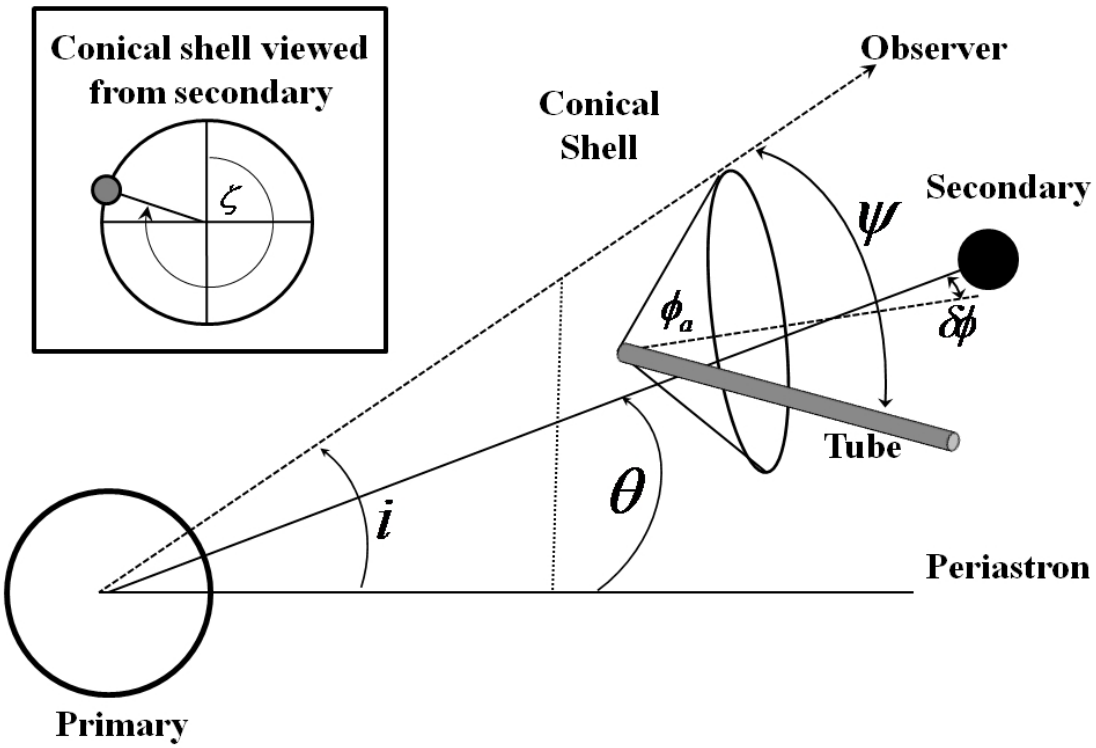

Fig. 2.— The geometry of the toy-model and definition of several parameters. The geometry is plotted near periastron ($\theta = 0$), where according to our model the secondary is toward us. An example of a "tube" is also shown. Both θ and $\delta\phi$ are measured in the equatorial plane. At each point along the orbit there is one value for each of the variables θ, $\delta\phi$, and ϕ_a, while we integrates over many tubes on the conical shell, each with its value of direction to the observed ψ.

Although the absorbing gas is a continuous media, we decompose the conical shell into 'tubes'. We define ζ to be the azimuthal angle on the surface of the conical shell; $\zeta = 0$ in a direction perpendicular to the equatorial plane, and is measured clockwise. Tubes exist from $\zeta = 0$ to $\zeta = 2\pi$. For each tube on the conical shell we calculate the angle ψ between the tube and the observer as a function of the orbital angle θ (see Figure 2)

$$\cos\psi = \cos\phi_a \sin i \cos(\theta - \delta\phi) + \sin\phi_a \sin\zeta \sin i \sin(\theta - \delta\phi) + \sin\phi_a \cos\zeta \cos i. \quad (6)$$

We take $v_0 < v_{\rm m} < v_{\rm max}$ to be the maximum velocity attended by a mass element, dm, in a tube; in each tube there is a large number of mass elements formed by the mixing process of the two winds. By mixing we refer also to secondary shocked wind segments that have been cooled to temperature low enough to contribute to the absorption at high speeds. They reside near the contact discontinuity as well. Here $v_0 = v_{1,\infty} = 500$ km s^{-1} is

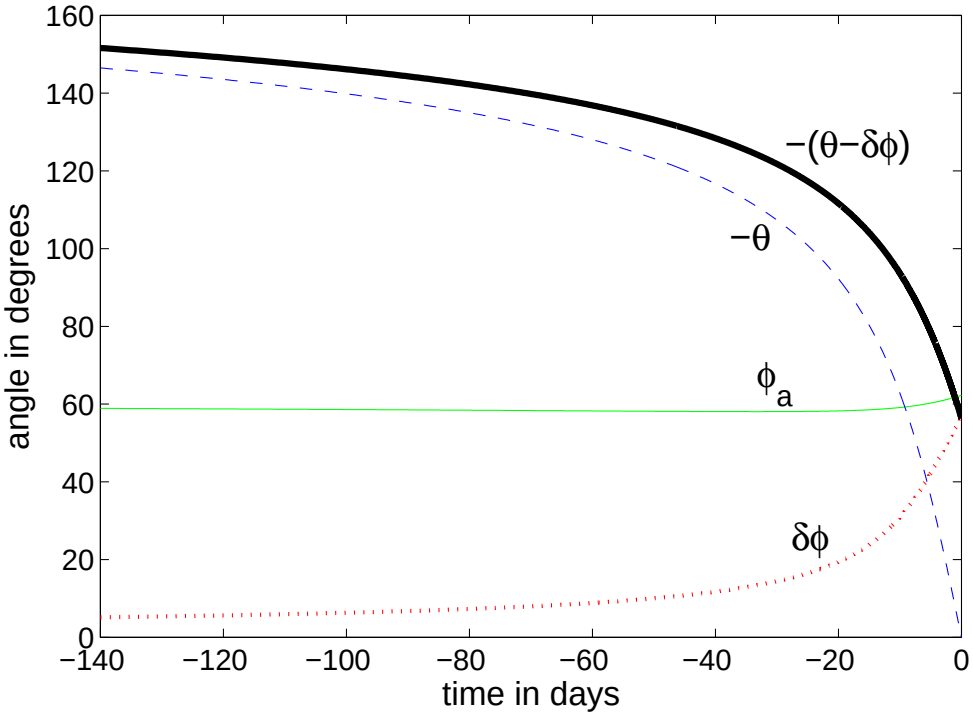

Fig. 3.— The time variation of angles defined in the text. θ is the orbital angle (line from primary to secondary) with $\theta = 0$ at periastron. $\delta\phi$ is the angle between two lines from the secondary: one to the primary star, and one to the stagnation point of the colliding winds. Both θ and $\delta\phi$ are measured in the equatorial plane. ϕ_a is the opening angle of the cone, defined around the cone axis.

the primary's wind velocity, and $v_{\rm max}$ is a parameter of the model that is constraint to be $v_{\rm max} \lesssim v_{2,\infty} = 3000$ km s^{-1}. The projected velocity of mass element having a velocity $v_{\rm m}$ and residing in a tube with an angle of ψ to our line of sight is $v_D = v_{\rm m} \cos\psi$.

Consider one of our tubes; it has a length L and a circular cross section with a radius R_t, such that $R_t \ll L$. The effective cross section of the absorbing tube is $2R_t L \sin\psi$. Therefore, the contribution of each tube to absorption is multiplied by $\sin\psi$. The amount of accelerated primary's wind to each velocity $v_{\rm m}$ is hard to predict. A numerical simulation beyond the scope of this work needs to be done in order to determine this amount. We simply take the velocity distribution to be constant, namely, in each tube the fraction of the gas in the velocity interval dv is constant $W(v)dv = C_W dv_m$, where C_W is a constant. Changing variable from the velocity along the tube to that along the line of sight, this weighting function (up to a constant) is, by using $v_D = v_{\rm m} \cos\psi$,

$$W(v_{\rm m})dv = W(v_D)dv_D = \frac{C_W}{\cos\psi} dv_D, \qquad (v_0 \cos\psi) < v_D < (v_{\rm max} \cos\psi). \tag{7}$$

At each orbital angle θ we sum the contribution to absorption at Doppler shift v_D over all tubes,

$$A(v_D) = \sum_{\text{tubes}} W(v_D) \sin\psi. \tag{8}$$

The intensity is taken to be

$$I(v_D, \theta) = 1 - K_a A(v_D, \theta), \tag{9}$$

where K_a is a constant of the toy-model that takes care of units and the condition $0 < I < 1$. We set here$K_a = 1/\max(\mathrm{A})$, because we do not compare to the absorption equivalent width.

Our model is actually a toy-model. It assumes a simple geometry of the absorbing material, i.e., a rotated conical shell with a varying opening angle, and a mass distribution within each tube that is constant with the velocity. The model contains two types of parameters: (1) Those that are given in the literature. Such are the binary parameters and the conical shape with its opening angle ϕ_a. These parameters are more or less in consensus. The orientation of the semimajor axis (the periastron longitude ω) is controversial, and we take the value from our previous papers $\omega = 90^\circ$ (secondary toward us at periastron). (2) Parameters that are unique to our toy-model. Such is the value of $v_{\max}$ which is constraint to be $v_{\max} \lesssim v_{2,\infty} = 3000$ km s^{-1}. For these parameters we find that a good general fit can be obtained for $v_{\max} = 2300$ km s^{-1}. The value of the absorption coefficient K_a has a small influence on our conclusions, and it serves only to give the general form of the absorption profile.

The assumption that the conical shell reaches its asymptotic opening angle at large distances breaks down as the system approaches periastron. The reason is that the relative velocity of the two stars is no longer much smaller than the primary's wind speed. This causes the winding-up of the conical shell into a spiral structure in the equatorial plane, e.g., as shown in the numerical study by Okazaki et al. (2008b). Only a close region near the binary system reaches this limiting angle. Namely, a smaller region, but much denser, will contribute to the absorption at the blue edge. However, contribution to the continuum near 1 μm comes from the stellar wind and hot dust from closer regions to the binary system (Kashi & Soker 2008a). Therefore, the much smaller region of the conical shell can still absorb a detectable fraction of the continuum. Our toy-model does not allow us to make any quantitative prediction. For that a 3D numerical code is required. Nevertheless, our toy-model does allow us to reach the two goals, as mentioned in the last paragraph of section 1.

4. THE BLUE ABSORPTION WING

In Figure 4 we present our results by a contour map of the intensity I, as given in equation 9, in the Doppler shift−time plane. The blue Doppler shift v_D is given in unit of km s^{-1}, and the vertical axis indicates days relative to (before) periastron (phase 0 at $t = 0$). The levels of the contours are $I = 1, 0.95, 0.9, 0.85, 0.8, 0.7, 0.6$, and so on, from left to right, where $I = 1$ indicates the edge of the absorption profile. Despite the constant weighting function W that we used, in reality we expect that the amount of helium blown with high velocities corresponding to $I \simeq 0.9 - 1$ will be too small to be detected. We have also estimated the velocity edges of the absorption wing at four epochs from Damineli et al. (2008b) observations; these are indicated by four horizontal error-bar lines,. The somewhat noisy data made it difficult to pinpoint the exact edge of the wing, and therefore we could only estimate it to an accuracy of ~ 100 km s^{-1}. Each line is centered at the approximated edges of the absorption wing, and extends to ± 50 km s^{-1} to each direction. At early times there is no noticeable differences between the contour lines in the range $I = 0.85 - 1$, and all nicely fit the two observation equally well. Very close to periastron, the line $I = 0.85$ fits the observations better. However, during this time we expect the collapse of the conical shell, such that no fresh gas will be accelerated to high velocities. We cannot make an accurate prediction so close to periastron passage. Over all, we consider the lines $I = 0.85 - 1$ to be a very good fit to observations.

We modified the parameters in our model to fit the observations of Damineli et al. (2008b) from the 2003 event. With this fitting we learn about two properties of the models. (1) We find that the orientation we use, where the secondary is toward us at periastron ($\omega = 90^\circ$) can account for the development of a wide blue absorption wing starting several months before periastron passage, if the absorbing material is within this conical shell. (2) According to our model, the maximum observed blue shift of the wing is reached ~ 5 day before periastron passage. The observed maximum blue shift might occur at a somewhat different time for three reasons. Firstly, the binary and winds parameters might be somewhat different than those we used. Secondly, we did not take into account the winding of the conical shell; we only considered the approximate direction of its axis by calculating the angle $\delta\phi$. Thirdly, close to periastron the conical shell is likely to collapse onto the secondary (Soker 2005; Kashi & Soker 2009).

With the only four available observations for the fitting, with the present possible degree of accuracy, and according to our parameters, we expect the maximum blue shifted absorption to occur $0 - 20$ day before periastron passage, i.e., late December or early January. There are two main reasons for that we cannot be more accurate. Firstly, we cannot treat properly the conical shell as the system approach periastron. Secondly, we expect the

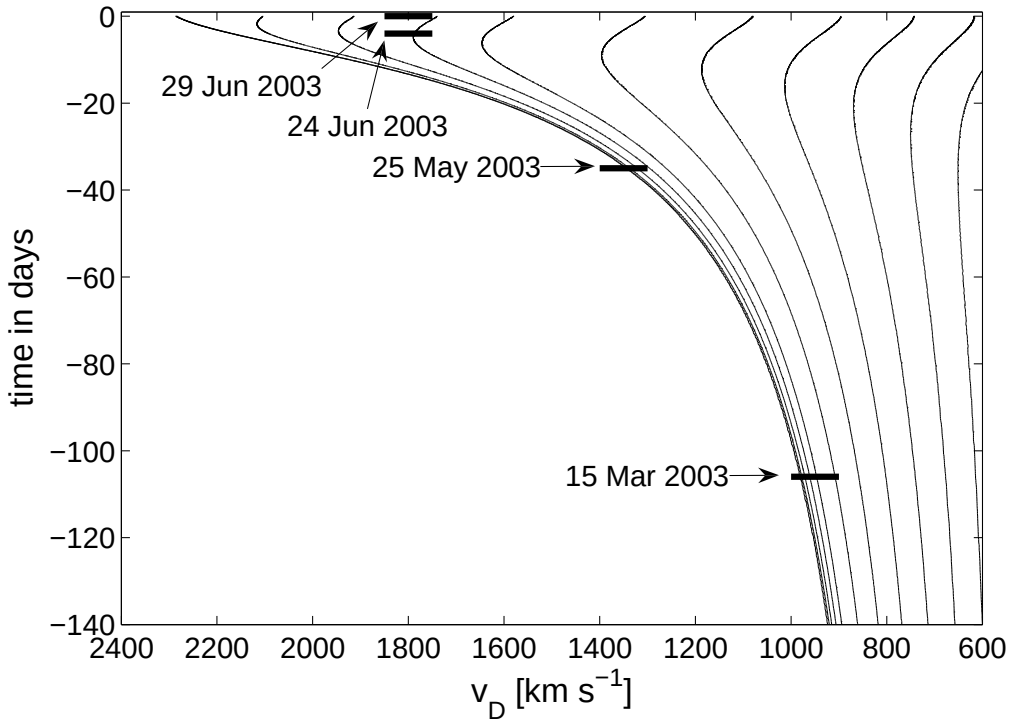

Fig. 4.— A contour map of the intensity I as given in equation 9, in the Doppler shift−time plane. The blue Doppler shift is given in unit of km s^{-1}, and the vertical axis indicates days before periastron (phase 0). The levels of the contours are $I = 1, 0.95, 0.9, 0.85, 0.8, 0.7, 0.6$, and so on, from left to right. The edges of the blue absorption wing at four epochs from Damineli et al. (2008b) are marked. The length of each of the drawn lines corresponds to 100 km s^{-1}, our estimate of the uncertainty in determining the edge of the absorption. We predict the edge Doppler shift to reach a maxima 0-20 days (according to our parameters) before periastron, when a maximum in v_D appears according to our model.

colliding wind region to collapse onto the secondary near periastron; we did not consider this process here either.

Our fundamental assumption is that the absorber of the blue wing of the He I λ10830Å line resides in the conical shell formed by the colliding winds. This assumption works quite well with the semimajor orientation $\omega = 90°$, where the secondary is closest to the observer at periastron passage. We now show that other orientations that are popular in the literature cannot account, not even qualitatively, for the behavior of the blue wing, if our fundamental assumption holds. We followed the calculations presented in Figure 4, but for three different semimajor axis orientations, as drawn in Figure 5: $\omega = 0$: The semimajor axis is perpendicular to the line of sight and the secondary is closer to the observer before the event. $\omega = 180°$: The semimajor axis is perpendicular to the line of sight and the secondary is closer to the

observer after the event. $\omega = 270°$: The secondary is closest to the observer at apastron, opposite to our favorite orientation of $\omega = 90°$ (Figure 4).

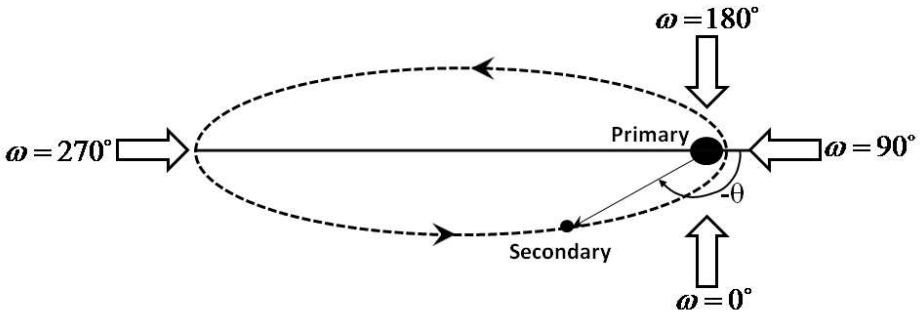

Fig. 5.— The fours semimajor orientations studied in the paper. In all cases the inclination angle (the angle between line of sight and a line perpendicular to the orbital plane) is $i = 41°$. Our favorite model has $\omega = 90°$, for which the blue absorption wing is drawn in figure 4.

The results for the expected Doppler shifts of the absorption wing are presented in Figure 6, together with the fours observations from Damineli et al. (2008b). It is clear that none of the other orientations can account for the observed absorption wing, not even qualitatively and just for the two early observations.

5. SUMMARY AND PREDICTION

We study the blue absorption wing of the He I λ10830Å P Cygni profile of η Car. The two winds of the two stars collide, and the post shocked gas of the two winds flow on both sides of a surface (the discontinuity surface) that has a pseudo-conical structure: the conical shell. The shocked secondary's wind accelerates part of the shocked primary's wind to high velocity (Figure 1). This gas, and the segments of the shocked secondary's wind which cool to a low temperature near the contact discontinuity (Figure 1), are assumed to be responsible

for the blue absorption wing. This is the fundamental assumption of our model. We use our previous results and assume an orientation where the secondary is toward the observer at periastron ($\omega = 90°$; see Figure 5). For the conical shell we built a toy model (Figure 2).

The absorption profile, up to a scaling factor, is calculated according to equations (8) and (9), and the results are presented in Figure 4. We are interested in the bluest part of the absorption profile, where intensity is lower; in our scaled units these are the contours in the range $I \simeq 0.8 - 1$. Using our fundamental assumption, and a toy model for the conical shell of the colliding winds, we showed that with our orbital orientation we can account for the appearance of the wide blue wing several months before periastron. Other semimajor orientations ω, cannot reproduce the results under our fundamental assumption (figure 6) This is our main result, namely, that if the absorber responsible for the blue wing of the He I λ10830Å line reside in the winds collision region, then only the $\omega \simeq 90°$ can account for the blue wing of this line.

Our results also predict that the Doppler shift v_D (the edge of the profile) will reach a maximum $0 - 3$ weeks before periastron passage. Since close to periastron the conical shell starts to collapse onto the primary, and even before it experiences the effect of wrapping, it is hard to pinpoint the exact time of this maximum. Nevertheless this maximum should be observed before the event.

We thank Augusto Damineli for providing us the observational data for the He I λ10830Å line, and an anonymous referee for helpful comments. This research was supported by the Asher Space Research Institute in the Technion.

REFERENCES

Abraham, Z., Falceta-Gonçalves, D., Dominici, T. P., Nyman, L.-A, Durouchoux, P., McAuliffe, F., Caproni, A., & Jatenco-Pereira, V. 2005, A&A, 437, 977

Akashi, M., Soker, N., & Behar, E. 2006, ApJ, 644.,451

Corcoran, M. F. 2005, AJ, 129, 2018

Corcoran, M. F., Ishibashi, K., Swank, J. H., & Petre, R., 2001, ApJ, 547, 1034

Corcoran, M. F., Pittard, J. M., Stevens, I. R., Henley, D. B., & Pollock, A. M. T. 2004, in the Proceedings of "X-Ray and Radio Connections",Santa Fe, NM, 3-6 February, 2004 (astro-ph/0406294)

Damineli, A. 1996, ApJ, 460L, 49D

Damineli, A., Corcoran M. F., Hillier, D. J. et al. 2008a, MNRAS, 386, 2330

Damineli, A., Hillier, D. J., Corcoran M. F. et al. 2008b MNRAS, 384, 1649

Damineli, A., Kaufer, A., Wolf, B., Stahl, O., Lopes, D. F., & de Araujo, F. X. 2000, ApJ, 528, L101

Damineli, A., Stahl, O., Kaufer, A., Wolf, B., Quast, G., and Lopes, D. F. 1998, 113, 299

Davidson, K. 1997 NewA, 2, 387D

Davidson, K., Martin, J., Humphreys, R. M., Ishibashi, K., Gull, T. R., Stahl, O., Weis, K., Hillier, D. J., Damineli, A., Corcoran, M., & Hamann, F. 2005, AJ, 129 900

Davidson, K., Smith, N., Gull, T.R., Ishibashi, K., & Hillier, D.J., 2001, AJ, 121, 1569.

Dorland, B. N., 2007, PhDT, 9D, "An Astrometric Analysis of Eta Carinae's Eruptive History Using HST WF/PC2 and ACS Observations"

Duncan, R. A., & White, S. M. 2003, MNRAS, 338, 425

Eichler, D., & Usov, V. 1993, ApJ, 402, 271

Falceta-Gonçalves, D., Jatenco-Pereira, V., & Abraham, Z. 2005, MNRAS, 357, 895

Henley, D. B., Corcoran, M. F., Pittard, J. M., Stevens, I. R., Hamaguchi, K., & Gull T. R. 2008, ApJ, 680, 705

Hill, G. M., Moffat, A. F. J., St-Louis, N. & Bartzakos, P. 2000, MNRAS, 318, 402H

Hillier, D. J., Davidson, K., Ishibashi, K., & Gull, T. 2001, ApJ, 553, 837

Hillier, D. J., Gull, T., Nielsen, K., Sonneborn, G., Iping, R., Smith, N., Corcoran, M., Damineli, A., Hamann, F. W., Martin, J. C., & Weis, K. 2006, ApJ, 642, 1098

Ishibashi, K., Corcoran, M. F., Davidson, K., Swank, J. H., Petre, R., Drake, S. A., Damineli, A., & White, S. 1999, ApJ, 524, 983

Kashi, A., & Soker, N. 2007a, MNRAS, 378, 1609

Kashi, A., & Soker, N. 2007b, NewA, 12, 590

Kashi, A., & Soker, N. 2008a, NewA, 13, 569

Kashi, A., & Soker, N. 2009, NewA, 14, 11

Kashi, A., & Soker, N. 2008b, MNRAS, 390, 1751

Luehrs, S. 1997, PASP, 109, 504

Martin, J. C., Davidson, K., Hamann, F., Stahl, O., & Weis, K. 2006a, PASP, 118, 697

Martin, J. C., Davidson, K., Humphreys, R. M., Hillier, D. J., & Ishibashi K. 2006b, ApJ, 640, 474

Nielsen, K. E., Corcoran, M. F., Gull T. R., Hillier, D. J., Hamaguchi, K., Ivarsson, S. & Lindler, D. J. 2007a, ApJ, 660, 669

Okazaki, A. T., Owocki, S. P., Russell, C. M. P., & Corcoran, M. F. 2008, MNRAS, 388, L39

Pittard, J. M. 2007, ApJ, 660, 141

Pittard, J. M., Corcoran, M. F. 2002, A&A 383 636P

Smith, N., Davidson, K., Gull, T.R., Ishibashi, K., & Hillier, D.J. 2003, ApJ, 586, 432

Smith, N. 2002, MNRAS, 337, 1252

Smith, N., Morse, J. A., Collins, N. R., & Gull, T. R. 2004, ApJ, 610, L105

Smith, N. 2006, ApJ, 644, 1151

Soker, N. 2005, ApJ, 635, 540

van Genderen A. M., Sterken, C., Allen, W. H., & Walker, W. S. G. 2006, JAD, 12, 3

Verner, E., Bruhweiler, F. & Gull, T. 2005, ApJ, 624, 973

Whitelock, P. A., Feast, M. W., Marang, F., & Breedt, E. 2004, MNRAS, 352, 447

Zanella, R., Wolf, B., & Stahl, O. 1984, A&A, 137, 79

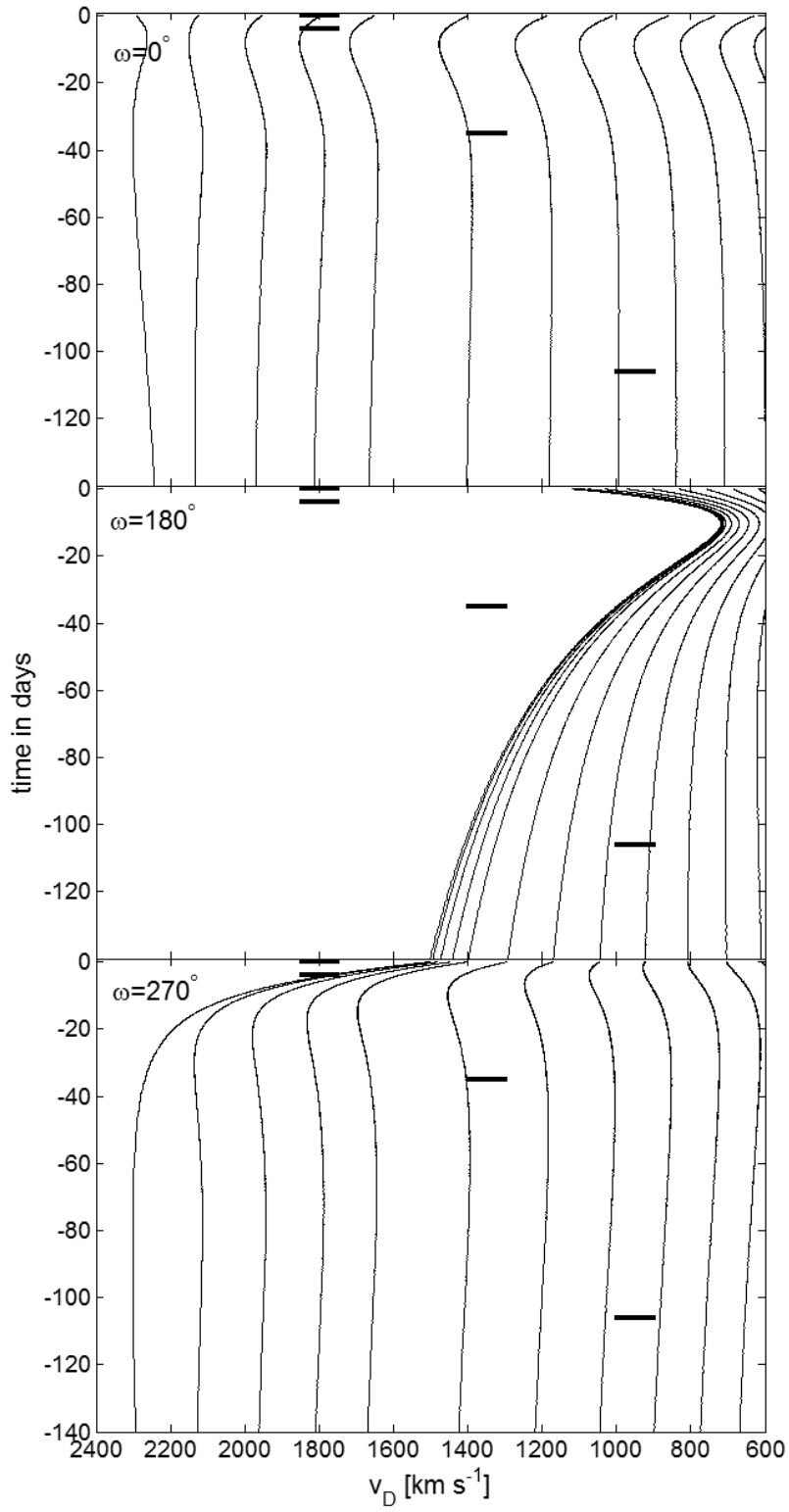

Fig. 6.— Same as in Figure 4, but for different values of ω, as schematically depicted in Figure 5 . None of the other orientations can account for the observed absorption wing under our fundamental assumption that the absorber reside in the conical region formed by the collision of the two winds. In particular, the opposite orientation, $\omega = 270°$, yields an entirely opposite behavior to observations, with minimum absorption at periastron.